

## Supplementary Information

# Manipulating the ambipolar characteristics of pentacene-based field-effect transistors

Liang-Yun Chiu,<sup>a</sup> Horng-Long Cheng,<sup>\*a</sup> Hsin-Yuan Wan,<sup>a</sup> Wei-Yang Chou<sup>a</sup> and Fu-Ching Tang<sup>b</sup>

<sup>a</sup> *Department of Photonics, Advanced Optoelectronic Technology Center, National Cheng Kung University, Tainan 701, Taiwan*

<sup>b</sup> *Department of Physics, National Cheng Kung University, Tainan 701, Taiwan*

### Corresponding Author

\*E-mail: [shlcheng@mail.ncku.edu.tw](mailto:shlcheng@mail.ncku.edu.tw)

## 1. Surface properties of gate dielectrics

**Table S1. Properties of polymer buffer layers on silicon dioxide (SiO<sub>2</sub>) gate dielectric and the corresponding interfacial tension ( $R_{12}$ )**

Gate dielectric or buffer	Thickness (nm)	Surface energy			Surface roughness (Å)	$R_{12}$ (mJ/m <sup>2</sup> )
		$\gamma^{d^a}$ (mJ/m <sup>2</sup> )	$\gamma^{p^a}$ (mJ/m <sup>2</sup> )	$\gamma$ (mJ/m <sup>2</sup> )		
SiO <sub>2</sub>	400	23.0	32.6	55.6	17.0	21.66
PVDF	42	30.4	15.7	46.1	19.1	6.16
PVNP	49	40.9	9.0	49.9	3.4	2.03
<i>h</i> -PMMA	426	33.3	8.1	41.4	2.7	1.80
PS	55	42.3	0.3	42.6	4.9	1.17
<i>t</i> -PMMA	188	33.7	6.1	39.7	3.8	0.95
<i>d</i> -PMMA	52	35.6	5.8	41.4	5.4	0.72
<i>ls</i> -PMMA	113	36.2	5.6	41.8	3.8	0.65
<i>hs</i> -PMMA	44	36.3	4.4	40.7	6.7	0.31
<i>s</i> -PMMA	63	36.8	3.7	40.5	4.0	0.14

<sup>a</sup>  $\gamma^d$  and  $\gamma^p$  denoted as the dispersion and polar force components of surface free energy, respectively.

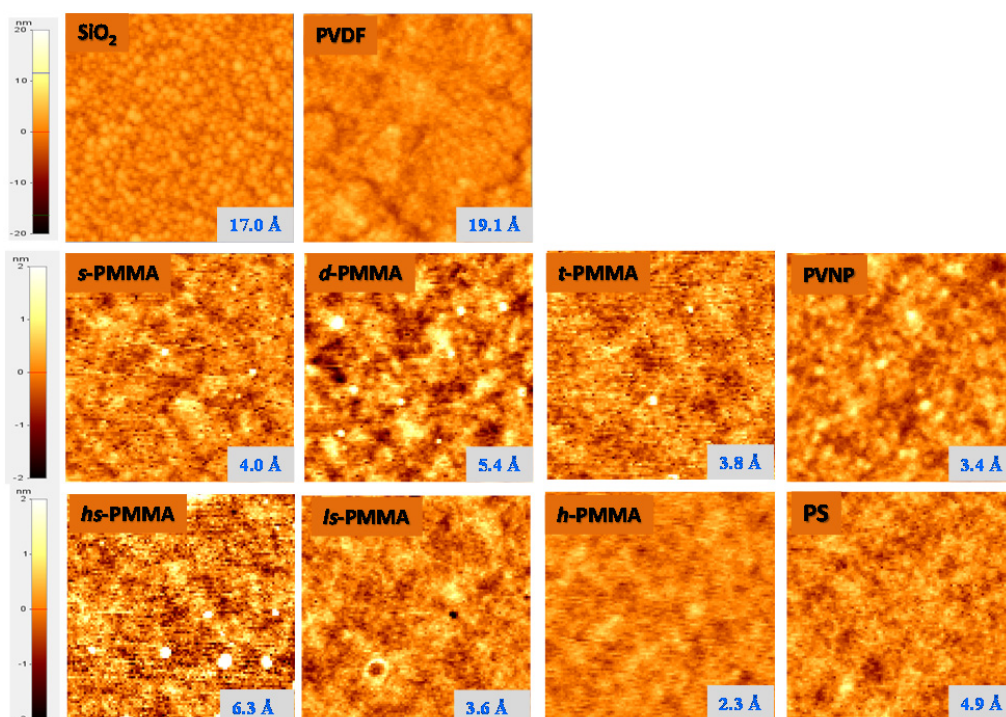


**Fig. S1** AFM images (2 μm x 2 μm) of SiO<sub>2</sub> and various polymer buffer layers. The root-mean-square roughness is also shown.

## 2. XRD and AFM analysis of other pentacene films

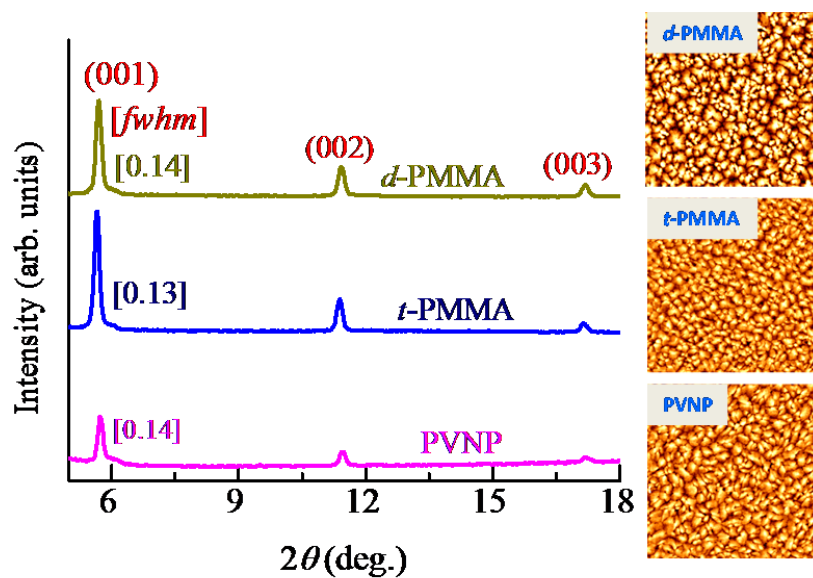


**Fig. S2** XRD pattern of the pentacene films (thickness of ca. 60 nm) on various surface-modified dielectrics. Note: the full width at half maximum (FWHM) of the (001) diffraction peak was also indicated. Inset: AFM images ( $5\ \mu\text{m} \times 5\ \mu\text{m}$ ) of the pentacene films with a thickness of ca. 10 nm.

### 3. Electrical characteristics of pentacene FETs and its complementary-like inverter

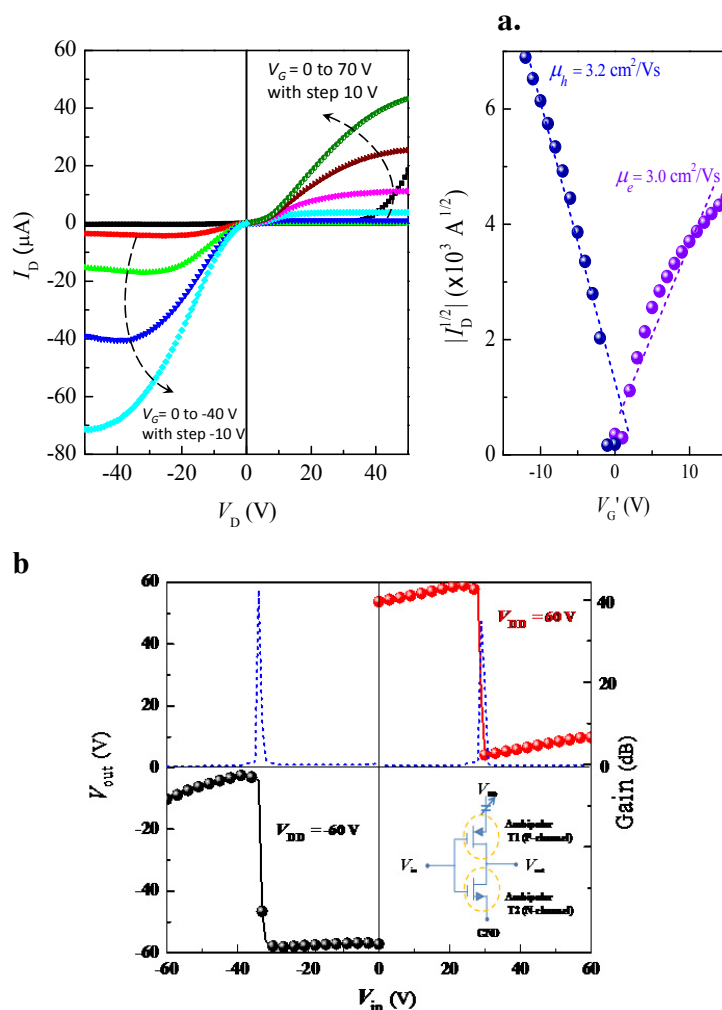


**Fig. S3** (a) *p*-Channel and *n*-channel electrical characteristics of pentacene FETs with *s*-PMMA surface-modified gate dielectrics. Left panel: output characteristics; Right panel: transfer characteristics.  $I_D$ : drain current,  $V_D$ : source-to-drain bias,  $V_G$ : gate bias, and  $V_G'$ : effective gate bias. (b) Transfer characteristics of complementary-like inverters based on two identical ambipolar pentacene FETs with *s*-PMMA surface modification. Depending on the polarity of the supply voltage  $V_{DD}$ , the inverter works in the first or the third quadrant. Top left and right (dashed lines): the corresponding signal gains. Inset bottom right: Schematic circuit configuration of a complementary-like inverter.

#### 4. Raman spectra

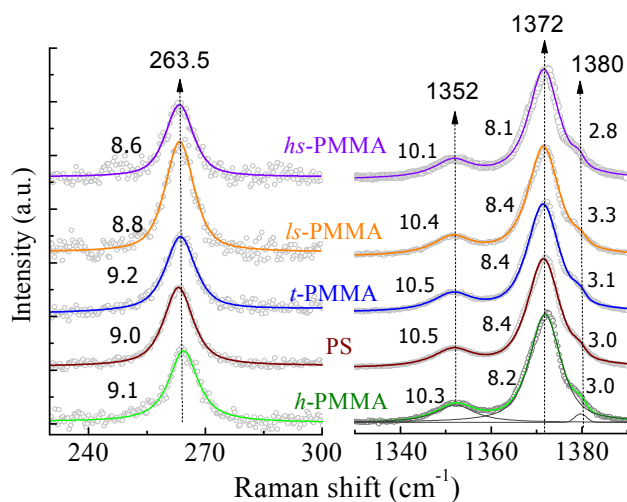


**Fig. S4** Raman spectra ( $\lambda_{exc} = 633$  nm) of the pentacene films (thickness of ca. 10 nm) grown on various dielectric surfaces. The spectra were normalized to the intensity of the 1371 cm<sup>-1</sup> band. The intensities of all spectra in left panel were enlarged ten times. The Gaussian/Lorentzian functions used for the deconvolution are presented by a thin solid line. The thick solid lines represent the overall fit, while the open cycles to the experimental data. The dashed lines serve as guidelines. Full width at half maximum (*fwhm*) of the selected bands are also shown.